PM$_{2.5}$ and ultrafine particulate matter emissions from natural gas-fired turbine for power generation☆

Eli Brewer [a], Yang Li [a], Bob Finken [b], Greg Quartucy [c], Lawrence Muzio [c], Al Baez [d], Mike Garibay [d], Heejung S. Jung [a, *]

[a] University of California Riverside (UCR), Department of Mechanical Engineering, Riverside, CA 92521, USA
[b] Delta Air Quality Services, Inc., 1845 North Case Street, Orange, CA 92865, USA
[c] Fossil Energy Research Corporation (FERCo), 23342-C South Pointe Dr., Laguna Hills, CA 92653, USA
[d] South Coast Air Quality Management District (SCAQMD), 21865 Copley Dr., Diamond Bar, CA 91765, USA

HIGHLIGHTS

- Emissions from the latest natural gas-fired turbine technologies.
- Tests include PM$_{2.5}$, wet chemical tests for SO$_2$/SO$_3$ & NH$_3$, and ultrafine PM.
- Strong presence of high concentrations of nanoparticles.
- Two orders of magnitude higher turbine particle emissions than background.

ARTICLE INFO

ABSTRACT

The generation of electricity from natural gas-fired turbines has increased more than 200% since 2003. In 2007 the South Coast Air Quality Management District (SCAQMD) funded a project to identify control strategies and technologies for PM$_{2.5}$ and ultrafine emissions from natural gas-fired turbine power plants and test at pilot scale advanced PM$_{2.5}$ technologies to reduce emissions from these gas turbine-based power plants. This prompted a study of the exhaust from new facilities to better understand air pollution in California. To characterize the emissions from new natural gas turbines, a series of tests were performed on a GE LMS100 gas turbine located at the Walnut Creek Energy Park in August 2013. These tests included particulate matter less than 2.5 μm in diameter (PM$_{2.5}$) and wet chemical tests for SO$_2$/SO$_3$ and NH$_3$, as well as ultrafine (less than 100 nm in diameter) particulate matter measurements. After turbine exhaust was diluted sevenfold with filtered air, particle concentrations in the 10−300 nm size range were approximately two orders of magnitude higher than those in the ambient air and those in the 2−3 nm size range were up to four orders of magnitude higher. This study also found that ammonia emissions were higher than expected, but in compliance with permit conditions. This was possibly due to an ammonia imbalance entering the catalyst, some flue gas bypassing the catalyst, or not enough catalyst volume. SO$_3$ accounted for an average of 23% of the total sulfur oxides emissions measured. While some of the SO$_3$ is formed in the combustion process, it is likely that the majority formed as the SO$_2$ in the combustion products passed across the oxidizing CO catalyst and SCR catalyst.

The 100 MW turbine sampled in this study emitted particle loadings of 3.63E-04 lb/MMBtu based on Methods 5.1/201A and 1.07E-04 lb/MMBtu based on SMPS method, which are similar to those previously measured from turbines in the SCAQMD area (FERCo et al., 2014), however, the turbine exhaust contained orders of magnitude higher particles than ambient air.

1. Introduction

Natural gas turbines (NGTs) are critical for meeting the demand of U.S. electrical power generation because they are uniquely suited to fulfill the energy gap left by hydroelectric, nuclear, and renewable energy sources. NGTs have a relatively quick start-up and shutdown time compared to other sources of electricity, making them ideal for supplying energy to the grid when the demand changes rapidly. New shale gas mining techniques have lowered the price of natural gas and allowed greater access to the United States' shale gas resources. The overnight capital cost (the cost of the project if no interest were accrued during its construction) of a NGT is low compared to other electrical generating sources (EIA, 2013b) and can be rapidly installed to cover unexpected situations like the shutdown of the San Onofre Nuclear Generating Station (Sewell, 2013).

Since 2003 California has seen an increase of over 200% in electrical generation from natural gas (CEC, 2014). The decreasing price and stable domestic supply of natural gas have strongly influenced its increased use, and the use of NGTs has been projected to increase until at least 2040 (EIA, 2013a). Studying the exhaust from these new facilities is critical to our understanding of air pollution in California.

Particulate Matter (PM) emissions from NGTs have been studied by several groups. England et al. (2007) investigated a compact dilution sampler (CDS) methodology to characterize fine particle emissions from stationary sources including three turbines. They found that the CDS method had lower detection limits compared to the regulatory methods for PM emissions. Tamura (2013) recently conducted a gap analysis of the filterable and condensable PM emission factors from stationary external and internal combustion sources fired by gaseous and liquid fuel to evaluate the accuracy of the sampling methodology. PM emission studies have covered many of the power plant combustors, however, there is still only limited research on emissions from aeroderivative turbines burning natural gas. Each fuel type emits a distinct chemical composition and particle range, based on combustion characteristics and the chemical nature of the fuel (Klippel et al., 2002; Mohr et al., 1995; Schmatloch, 2000). NGTs emit a wide range of particles, however PM is regulated on a mass concentration basis (SCAQMD, 2002) and the vast majority of particles from combustion sources are in the nanometer range. Ultrafine PM (particles < 100 nm in diameter) has not been regulated separately by the EPA.

Ultrafine particles have recently become a cause for concern, as our understanding of their effect on the human body has improved. They were hypothesized to have potentially increased health risks from those of larger particles due to their higher lung deposition rate, clearance mechanism, and ability to translocate to extrapulmonary locations e.g. lymph, and blood circulation (Elder and Oberdörster, 2005). Current knowledge on the health effects of ultrafine PM are uncertain. A Health Effects Institute review in 2013 concluded that the state of science was inconclusive regarding the toxicity of ultrafine PM due to inconsistencies and limitations in the findings from both short- and long-term studies (HEI, 2013). Current U.S. EPA regulations measure $PM_{2.5}$ emissions using mass based methods, however larger particles, which are usually generated by incomplete combustion, make up a much higher mass fraction than ultrafine particles.

SCAQMD funded a two stage project to technically and economically assess a variety of control strategies and technologies that could potentially be used to reduce $PM_{2.5}$ and ultrafine emissions from NGT power plants. In 2007 SCAQMD amended rule 1309.1 to allow prospective gas turbine-based power plants conditional access to its Priority Reserve account to procure reduction credits to offset $PM_{2.5}$ emissions. At the same time, SCAQMD initiated a project to identify and test at pilot scale advanced $PM_{2.5}$ technologies to reduce emissions from these gas turbine-based power plants. The first phase (FERCo et al., 2009) of this project entailed an assessment of technologies to reduce $PM_{2.5}$ and ultrafine particles from gas turbine engines; the second phase (FERCo et al., 2014) of the project entailed pilot scale evaluations of technologies recommended from the first phase. This paper reports part of the results from the second phase of the project with the main objective of characterizing and quantifying $PM_{2.5}$ and ultrafine particles that are emitted by modern aeroderivative NGTs during daily operation. The $PM_{2.5}$ test methods selected for this project were chosen from currently available methods. SCAQMD Method 5.1 (1989) combined with EPA Method 201A (2010) were chosen as the test methods because recent projects in the SCAQMD jurisdiction have utilized this combination of methods for the determination of $PM_{2.5}$ including condensable PM. Methods 5.1/201A are detailed in section 2.2.2.

2. Experimental

2.1. Test site, turbine, fuel, and lubricant

Tests were conducted at the Walnut Creek Energy Park (WCEP) in the City of Industry, CA in August 2013. The test site was selected because it was representative of new aeroderivative turbines and had the newest commercial NO_x control system. WCEP was designed as a peaking plant to provide electrical generation during high demand periods i.e. Southern California's hot summer months.

WCEP consists of five GE LMS100 combustion turbines in simple cycle operation. The LMS100 is an aeroderivative gas turbine rated nominally at 100 MW (GE, 2015). The LMS100 derives its high efficiency and increased power output from its innovative intercooling system between the low-pressure and high-pressure compressors. WCEP uses reclaimed water for cooling; each LMS100 employs Selective Catalytic Reduction (SCR) system (from Haldor-Topsoe), using aqueous ammonia as the reagent, and water injection for NO_x control. They are also equipped with a CO catalyst (from BASF). The test unit for this study was WCEP Unit 2 and its exhaust layout is shown in Fig. 1.
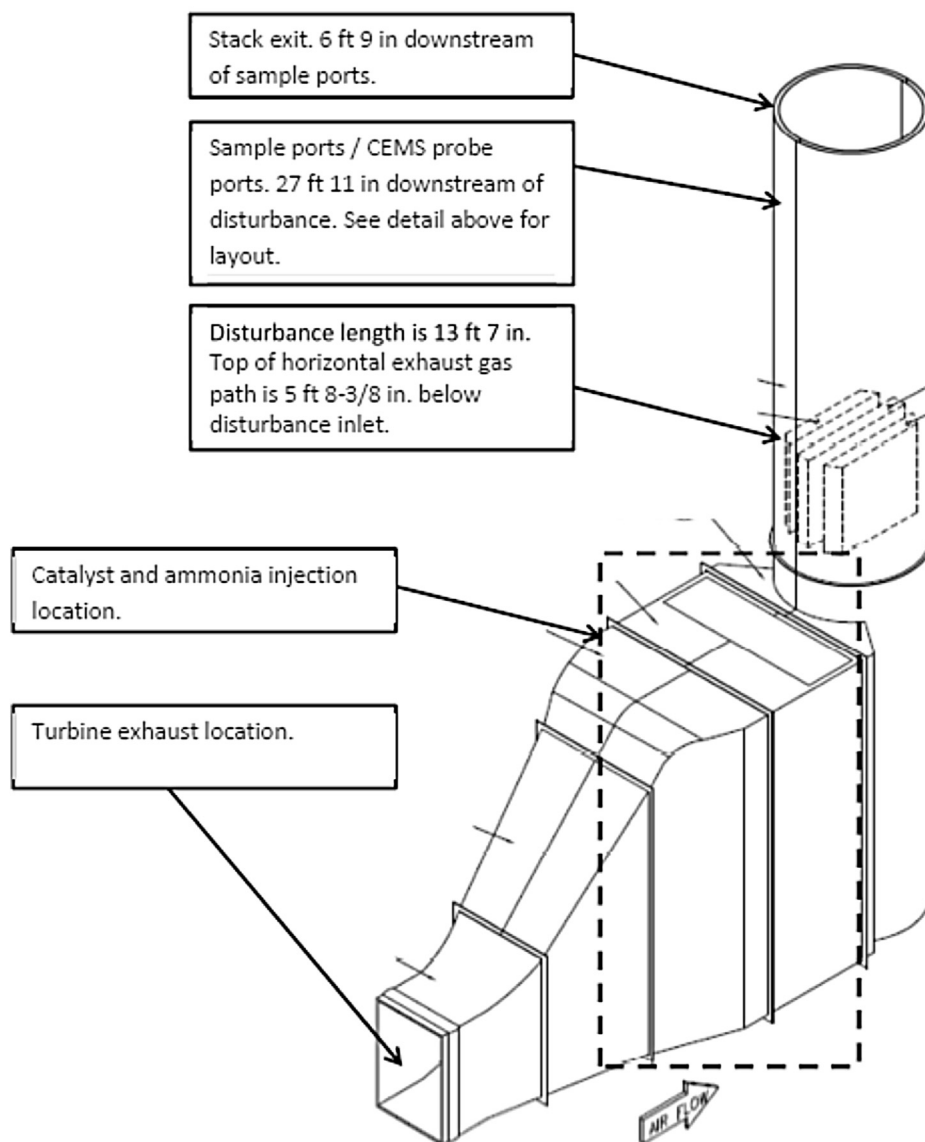
Specific fuel analysis was not performed for this study. In general, the average Wobbe number for California pipeline natural gas is in the range of 1335–1340 Btu/scf with sulfur content in the range of 0.25–1 grain/100scf (CEC, 2008). The LMS 100s at WCEP uses two types of oil: Mobil DTE Light lubrication oil and Mobil Jet Oil II.

The ultrafine PM tests were conducted before turbine operation, during plant warm-up, and during normal operation. A record was kept of which turbines were running to track how ambient conditions changed with energy park operation. WCEP is located adjacent to a train yard and the associated diesel locomotive traffic influenced the ambient conditions. Energy park operation is controlled by Southern California Edison (SCE) and is dictated by the demand on the electrical grid.

2.2. Measurement setup

2.2.1. Ultrafine particle measurement setup

Samples were pulled from the middle of the stack through an unheated, uninsulated, 73″ long, 3/8″ stainless steel tube inserted into a sample port that was located on the side of the stack above the platform. The sample probe was connected via silicon conductive tubing to a critical orifice upstream of an ejector pump (Air-Vac, model TD110H). A mixing tunnel was connected downstream of the ejector pump to mix the dilution air with the sample maintaining a dilution ratio of 7.1:1. Dimensions and details of the

SIMPLIFIED EXHAUST STACK DIAGRAM

Stack exit. 6 ft 9 in downstream of sample ports.

Sample ports / CEMS probe ports. 27 ft 11 in downstream of disturbance. See detail above for layout.

Disturbance length is 13 ft 7 in. Top of horizontal exhaust gas path is 5 ft 8-3/8 in. below disturbance inlet.

Catalyst and ammonia injection location.

Turbine exhaust location.

AIR FLOW

Notes:

1. Stack inside diameter is 13'-6".
2. Overall stack height is 90'-0".

Fig. 1. WCEP unit 2 stack diagram.

mixing tunnel can be found at the reference (Abdul-Khalek, 1996). Compressed air (maintained at 30 *psi*) was supplied by the power plant and filtered to particle free air by a clean air system (TSI model 3074). The ultrafine particle measurement setup (seen in Fig. 2) had the sample passing through the dilution tunnel to the SMPS (TSI model 3936), EAD (TSI model 3070A), Transmission Electron Microscope (TEM) sampler, and Catalytic Stripper (CS). The thermo-phoretic TEM sampler separately directly sampled the turbine exhaust. The CS was connected in-line, before the SMPS, during part of the tests to determine a portion of the sample that was made of Volatile Organic Compounds (VOCs).

Two types of classifiers were used for the SMPS: the long column DMA (model 3081) sampled over a range of 7–290 nm, and the Nano DMA (model 3085) sampled over a range of 2.5–80 nm. The SMPS used an ultrafine Condensation Particle Counter (TSI, CPC 3776), which has a cut point of 2.5 nm. Due to the warm ambient temperatures during the test, the CPC was placed in a small cardboard box where a portable air conditioner supplied cool air. This was necessary to keep the CPC's condenser temperature below its operating maximum.
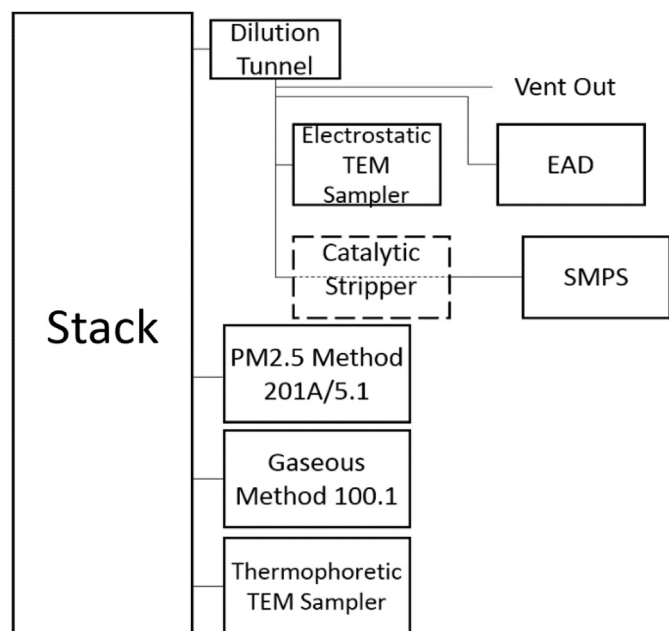
Fig. 2. Experimental setup diagram, the Catalytic Stripper was used only on certain tests, and when it was not used the SMPS received a direct line from the diluted sample. It should be noted that a thermophoretic TEM sampler was used to directly sample stack flow.

Two types of samplers were used to collect particles on TEM grids. The thermophoretic sampler was inserted into the stack with a residence time of a fraction of a second. A guiding tube was used so that the TEM grids were only exposed to particles in the stack. This is the same thermophoretic sampler used by Murphy et al. (2009). The electrostatic particle sampler (FHNW TEM Sampler, Switzerland) was also used to collect particle samples after the sample flow was diluted. Typical sampling time ranged from 30 to 120 min for the electrostatic particle sampler. Both Silicon Oxide (SiO) and Carbon coated 200 mesh copper grids were used.

A custom built CS (similar in design to Abdul-Khalek and Kittelson (1995), and Stenitzer (2003)) was used in-line upstream of the SMPS to measure the fraction of the PM that were Volatile Organic Compounds (VOCs). The CS has two catalysts that are heated to 300 °C: the first oxidizes hydrocarbon components (Oxicat), and the second removes sulfur components (S-trap) from the sample flow. The sample flow passes through a cooling coil to decrease the flow to ambient temperature before exiting the CS. A flow rate of 1.5 lpm was used to match the flow rate of the SMPS, and thermophoretic and diffusion losses were accounted for.

The EAD detects diameter concentration load using the principle of diffusion charging. It then calculates the concentration based on a TSI propriety linear relationship. Diameter concentration is correlated with the degree that tracheobronchial and alveolar regions have been covered by ultrafine particles (TSI, 2012; Wilson et al., 2007).

2.2.2. $PM_{2.5}$ measurement setup

$PM_{2.5}$ was measured using both U.S. EPA method 201A/SCAQMD method 5.1 and U.S. EPA methods 201A/202 for the SCAQMD project. This paper mainly reports results by method 201A/5.1, however, the full report (FERCo et al., 2014) contains results by the other method that are outside the scope of this paper. For more details see the full report. Method 201A/5.1 was further explained in the supplemental document along with Fig. S1.

Sampling times for the Method 201A/5.1 tests ranged from 4.04

to 8.38 h, and averaged 6.23 h. Meter sampling volumes averaged 161.7 scf and varied from 106.4 to 219.5 scf. Sample times for the Method 201A/202 tests ranged from 4.09 to 8.27 h and averaged 6.01 h. Corresponding sample volumes varied from 108.2 to 223.5 scf and averaged 160.4 scf. One field blank was collected and daily reagent blanks were collected with each $PM_{2.5}$ sample. Average $PM_{2.5}$ mass was 3–10 times larger than field and reagent blanks for Method 201A/5.1.

2.2.3. Gas measurement setup

NO_x, CO, O_2 and CO_2 concentrations were measured using SCAQMD Method 100.1 and a dry extractive continuous emissions monitoring (CEM) system. The CEM has a heated probe, a heat traced Teflon sample line connected to a thermo-electrically cooled sample dryer to minimize loss of NO_2. The gas analysis portion is composed of a chemiluminescent NO_x analyzer (CAI Model 600), a gas filter correlation CO analyzer (Thermo-Fisher Model 48i), an electrochemical O_2 analyzer (AMI Model 201), and a non-dispersive infrared CO_2 analyzer (Horiba Model PIR-2000). A low temperature carbon converter was used to convert NO_2 to NO for measurement of total NO_x and converter efficiency was tested daily.

The ammonia slip (the amount of ammonia that escapes the SCR system unreacted) was measured using SCAQMD Method 207.1 (shown and detailed in Fig. S2). NCASI Method 8A was used to measure the concentrations of SO_2 and SO_3 (see and detailed in Fig. S3).

3. Results and discussion

3.1. Particle size distributions and morphology

Fig. 3 shows the average SMPS results using both the Long and Nano DMA columns. Ambient particle size distributions are shown as averages of five test days and turbine exhaust particle size distributions are averages of two test days. Due to the relatively low dilution ratio, the sampling condition was close to the ion depletion condition of the bipolar neutralizer on the SMPS. The data were screened to ensure that the measurements presented in this paper were not conducted under the ion depletion condition, averaged data are also provided in Fig. S4. The SMPS data shows good agreement over the range of overlap between 7 nm and 80 nm. The particle size distribution of the exhaust showed a bimodal distribution, with peaks around 2.8 and 17 nm. The ultrafine particle emissions from the stack were at least an order of magnitude higher than ambient air over the entire size range. At the 100 nm size, stack particle concentrations were 20 times higher than ambient particle concentrations. This increased to an average of 3.9×10^4 times higher in the 2.5–3 nm range. Overall, dilution ratio corrected stack particle concentrations were over 6.9×10^2 times higher than ambient particle concentrations. Total ambient particle concentrations were in the range of 3.5×10^4 particles/cm^3, which is higher than typical background particle concentration in the region. It should be noted that England et al. (2007) reported particle size distribution and total concentration were affected by dilution ratio when it was lower than 20:1. In general this dependence is source specific and further investigation at higher dilution ratio will warrant representativeness of the particle size distribution presented in this study.

Nguyen and Jung (2015) has reported total ambient particle concentrations of 8×10^3–10^4 particles/cm^3 for a background location in Riverside California, while others have reported higher total ambient particle concentrations of ~10^4–10^5 particles/cm^3 for measurements taken near a major highway (Grady et al., 2013; Zhu et al., 2007). Total ambient particle concentrations are higher than expected for an urban area and this is attributed to the close
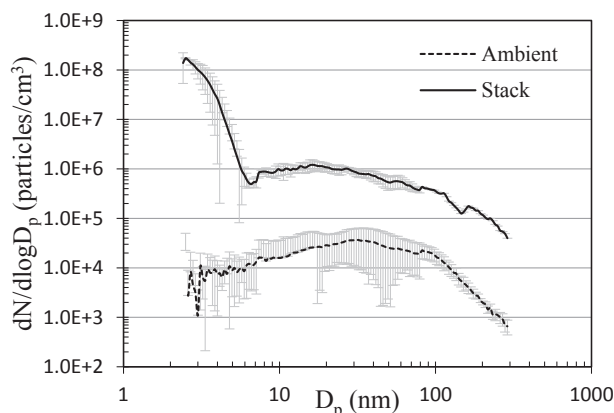
Fig. 3. Particle size distributions from the stack of the turbine engine in comparison to those from ambient air. Particle concentrations were corrected for dilution ratio. Total stack and ambient concentrations are 2.4×10^7 and 3.5×10^4 particles/cm^3 respectively.

proximity (less than a kilometer) to a major highway (California State Route 60) and the adjacent train yard. The results of our study contradict what Klippel et al. (2002, 2004) reported that gas-fired turbine exhaust particle concentrations were lower than those of ambient air. They found similar results for both 260 MW and 7.9 MW turbines. The 260 MW turbine has water injection for NO_x control, similar to the turbine sampled in this study. They did not measure particles below 10 nm, therefore the presence of nanoparticles in the exhaust of their turbines cannot be ruled out. Their particle size distributions show significantly lower accumulation mode (>30 nm in diameter) particle concentrations than those in this study. We speculate that the post combustion temperatures of their turbines were much higher than those of the turbine sampled in this study, leading to further oxidation or gasification of accumulation mode particles. Information on the sulfur content of the fuel could provide an improved explanation of nucleation mode particles (<30 nm in diameter), however, neither of the studies measured fuel sulfur content. It should be noted that the dilution ratio of the Klippel (2002, 2004)'s study was 75 which was 10 times higher than this study.

The CS was inserted between the dilution tunnel and the SMPS to remove semi-volatiles and sulfur compounds from the aerosol sample streams in order to quantify the amount of VOCs in the exhaust. The fraction of particles that were semi-volatile can be determined from the difference between cold and hot particle counts (accounting for thermophoretic and diffusion losses). Thermophoretic losses are less dependent on particle size than diffusion losses (for particle sizes between 10 and 100 nm). Size independent thermophoretic losses were not observed in our measurements for particles between 10 and 40 nm. We assume that a fraction of the 100 nm particles were semi-volatile because of the lower particle counts measured downstream of the hot CS in that size range (see Fig. S5). Further study is required to confirm this observation due to a lack of robust CS test data and high diffusion losses within the CS.

Researches have investigated particle size distributions from combustion sources and have found a variety of factors that impact the shape of the distribution. Gysel et al. (2015) varied the dilution conditions (temperature, humidity, and residence time) of nucleation mode particles from a NGT and showed that they were highly hygroscopic, and sulfur compounds in the exhaust combined with the various dilution conditions could significantly affect the peak diameter of the particles. Wey et al. (2007) reported that particle size distributions from aircraft turbine burning jet fuels. Their

particle size distributions were different compared to our study. Lobo et al. (2011) reported unimodal particle size distributions with the mode diameters ranging from 20 to 30 nm, while Herndon et al. (2008) reported bimodal particle size distributions with the mode of the nucleation mode around 10 nm and the larger peak in the 40—70 nm range. England and McGrath (2004) showed particle size distributions measured by SMPS from a 48 MW aeroderivative cogeneration turbine burning refinery fuel. They reported bimodal particle size distributions which are similar to the current study. However the concentrations of their particle size distributions were much lower. They reported 1.8×10^5 to 3.5×10^5 particles/cm^3 in total particle concentration. Nucleation mode diameters were around 20 nm and nucleation mode concentrations accounted for ~98% of total number count. Chang and England (2004) showed particle size distribution measured by SMPS, and PM measured by Method 201A/202 for a 234 kW pilot scale combustion facility, which is significantly different from the aeroderivative turbine in this study. Wien et al. (2004), and England et al. (2004) measured PM with methods 201A/202 on a 240 and 554 MW, respectively, cogenerative supplementary-fired natural gas combined cycle power plants, which is a different type of turbine. England et al. (2007) found that both residence time and dilution ratio affect the particle distribution from burning natural gas, however these changes were all within the same order of magnitude. These papers have distinct differences from this study and cannot be directly compared with the result of this study.

This study found significant concentrations of nanoparticles with smaller peak diameter than those found in the emissions from jet fuels. Despite the relatively short lifetime (minutes to hours) of nanoparticles in the atmosphere, they can become a concern for public health when they coagulate onto accumulation mode particles, which have lifetimes on the order of days (Buseck and Adachi, 2008; Friedlander, 2000).

TEM samples were taken to study the morphology and chemical composition of particles emitted from the turbine. These grids were analyzed on a Philips CM300 TEM at UCR's Central Facility for Advanced Microscopy and Microanalysis (CFAMM). Four TEM images of the particles are shown in Fig. 4. There is a consistently dominant presence of 2—3 nm diameter particles due to the significantly higher concentration (four orders of magnitude) of nanoparticles in the turbine exhaust. Although a few larger particles were observed, they were not photographed due to our interest in the smaller particles. Energy-dispersive X-ray spectroscopy (EDX) analysis was inconclusive because the volume of nanoparticles was small and the signal to noise ratio was low. The low contrast particles shown in Fig. 4 are assumed to be non-metallic because metal particles typically have high contrast in TEM images. It is unlikely that the particles seen on the TEM grids were semi-volatile due to the presence of a CO catalyst in the turbine (the CO catalyst is designed to remove hydrocarbons, much like our CS). Further testing is necessary to determine their exact chemical composition and formation process.

The particle mass concentration was estimated based on the particle size distribution. Two different effective density profiles for particles were used and results are shown in Fig. S6. Initially, a constant density of 1 g/cm^3 was used (assuming a spherical particle shape). Most organic aerosols have densities in the range from 1.22 to 1.43 g/cm^3 (Kuwata et al., 2011; Nakao et al., 2013), while representative particle phase inorganics (e.g. ammonium nitrate and ammonium sulfate) have densities of 1.72 and 1.77 g/cm^3 respectively. The effective density distribution from Maricq and Xu (2004) was utilized for accumulation mode particles as shown in Equation (1). A density of 1.46 g/cm^3 (equal to that of hydrated sulfuric acid) was assumed following Zheng et al.'s (2012) calculation for nucleation mode particles.
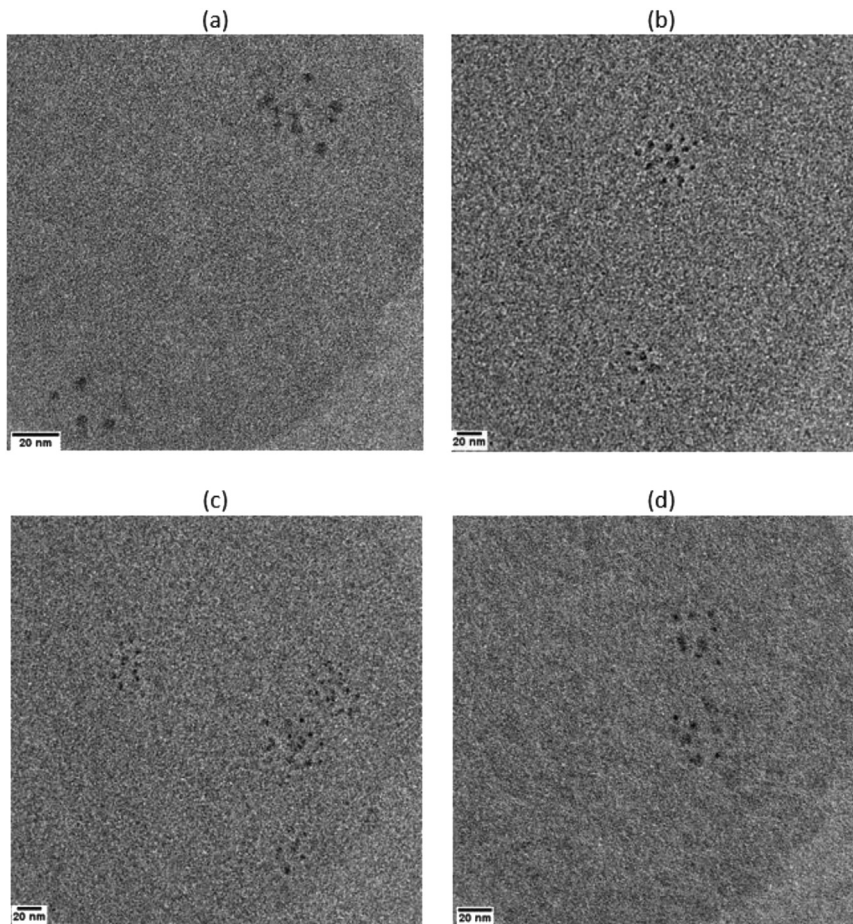
Fig. 4. TEM images of sampled particles from unit 2 by thermophoretic TEM sampler (a) Day 6 (b) Day 7 (c) Day 8 (d) Day 9.

$$\rho_{eff} = 1.2378*e^{-0.048D_p} \ (D_p > 30 \text{ nm}) \qquad \text{Equation 1}$$

Integration of the particle mass, obtained from each size bin, yielded an ambient PM mass of 5.7 μg/m^3 (for a constant density of 1 g/cc), and 4.0 μg/m^3 (for the complex density profile). Our calculation was approximately in the similar range with the air quality index (AQI) reported during the test days (49 ± 2.7, or 11.75 ± 0.57 μg/m^3).

The CPC and EAD were used to monitor changes in particle number and diameter concentration during the load variations (see Table S1 for operating data summary and details). The CPC periodically counted sample flow (bypassing the SMPS), however the sample flow often surpassed the instrument's concentration limit because of the high particle concentration of the turbine exhaust and useful monitoring data could not be obtained. The EAD recorded the transient response of particle emissions from the stack during the load variations (Fig. 5). While particle emissions decreased with no time-delay when the load decreased from 100 to 50 MW, there was a 10—15 min time-delay when the load was increased from 50 to 100 MW. There were spikes in the particle concentration when the turbine operated at either 50 MW or 100 MW. It should be noted that the EAD has low penetration and charging efficiencies for particles below 10 nm, however we speculate that the EAD may have responded to sub-10 nm particles because of the high concentrations recorded.

3.2. PM$_{2.5}$ measured by the method 201A/5.1

The loading of PM$_{2.5}$ in the exhaust, measured using Method

201A/5.1 (Table 1), was 0.000296 grain/dscf (677 μg/m^3). Of the total PM$_{2.5}$: 8.1% (55 μg/m^3) was condensable organic PM, 84.8% (574 μg/m^3) was condensable inorganic PM, and 7.1% (48 μg/m^3) was solid PM$_{2.5}$ (Fig. 6). The PM mass estimated from particle size distributions (assuming a unit density) was 200 μg/m^3, and is on the same order of magnitude to the 654 μg/m^3 of PM measured by the Method 201A/5.1. It should be noted the difference may have come from uncertainties in particle effective density and condensable PM captured by the Method 201A/5.1. The SMPS-derived
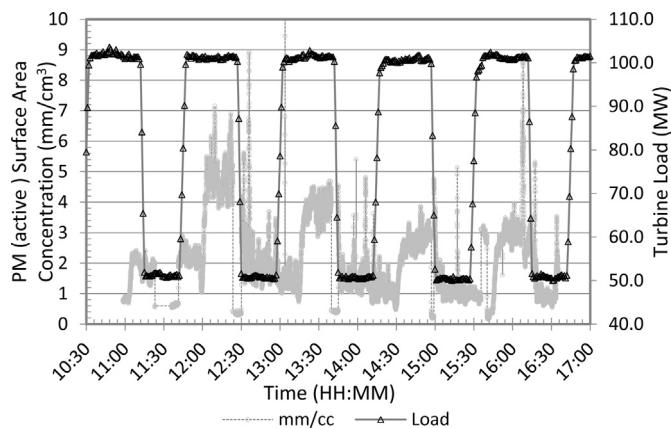

Fig. 5. EAD aerosol diameter concentration vs varying turbine load.

mass emission factor (200 μg/m^3 = 1.07E-04 lb/MMBtu) was comparable to the dilution sampling data of England (2004) (See their Tables 3 and 4) which were taken from several tests conducted on gas turbines equipped with SCR and oxidation catalysts. The impinger based data (677 μg/m^3 = 3.63E-04 lb/MMBtu and 654 μg/m^3 = 3.51E-04 lb/MMBtu) appear to agree with the impinger-based data summarized by Tamura (2013) in their Figs. 4-1. These values are much lower than those emission factors in AP-42 (EPA, 2015), which are still commonly used.

Ionic analyses were performed for seven anions (sulfate, chloride, fluoride, nitrite, nitrate, bromide, and phosphate) and six cations (ammonium, calcium, lithium, magnesium, potassium, and sodium) for the impinger catch solutions to examine chemical composition of condensable inorganic PM.

Sulfate was the largest fraction of the condensable inorganic PM$_{2.5}$ (averaging around 47%, Fig. 7), ammonium accounted for 12%, and sodium accounted for 4.4%. Chloride, nitrate, fluoride, bromide, potassium, calcium, lithium, and magnesium were present in small quantities. The remaining portion of the condensable inorganic PM (29%) could not be identified. The large contributions of ammonium and sulfate to the total PM$_{2.5}$ indicate that control of these two species could significantly reduce PM$_{2.5}$ emissions from NGT power plants. Further analysis gives insight to the nature of PM. The stack SO$_3$ concentration (0.017 ppmv) is equivalent to ~90 μg/m^3 as either H$_2$SO$_4$(H$_2$O)$_2$ or (NH$_4$)$_2$SO$_4$ as SO$_3$ reacts with H$_2$O and converts to H$_2$SO$_4$ very quickly at these stack temperatures and moisture concentrations. This is about twice of the solid PM measured with Method 201A/5.1 suggesting half of the SO$_3$ was captured onto the filter while the rest ended up in the impingers. The proportion of ammonium and sulfate in the impinge catch shown in Fig. 7 suggests ammonium sulfate. Stack SO$_2$ concentration is equivalent to about 330 μg/m^3 as ammonium sulfate. Adding SO$_3$ in the impinger catch leads to total 370 μg/m^3 ammonium sulfate. This suggests that much of the inorganic condensable PM measured with Method 201A/5.1 could be explained by capture of SO$_2$ and conversion to ammonium sulfate within the impinger.

The water in the exhaust was also analyzed to determine whether water injected into the system affected PM. Water condensed in the impingers included the injected water, the water formed when natural gas was burned, and a small amount (about 0.1%) of dilution water from the aqueous ammonia. On average, the injected water accounted for 22% of the total water in the combustion products. Anion analysis of the injection water indicated concentrations of sulfate, chloride, and total nitrogen (i.e. nitrites and nitrates) were 0.099, 0.068, and 0.30 ppm respectively. No fluoride, bromide, or phosphate was found.

Total organic carbon (TOC) was measured from the impinger catch solution using a GE Sievers 900 portable TOC analyzer. TOC was obtained by subtracting total inorganic carbon (TIC) from total carbon. TOC averaged 5.4 ppm while TIC was much lower, averaging 0.18 ppm.

The result from Method 201A/202 showed a similar trend to those from the Method 201A/5.1. Detailed comparison of the results by the two methods are beyond the scope of this paper. Readers who are interested in this comparison should see our report (FERCo
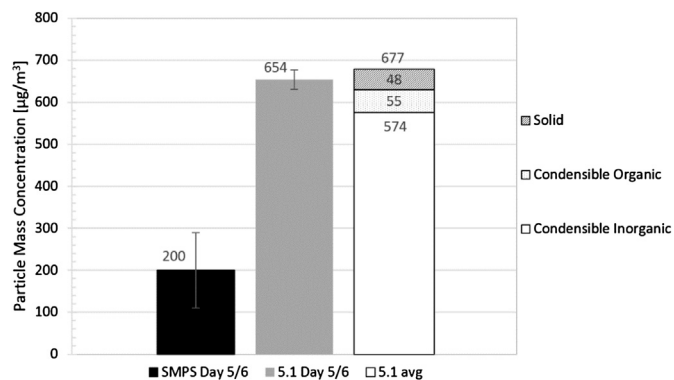

Fig. 6. PM$_{2.5}$ measured using SMPS, Methods 201A/5.1.

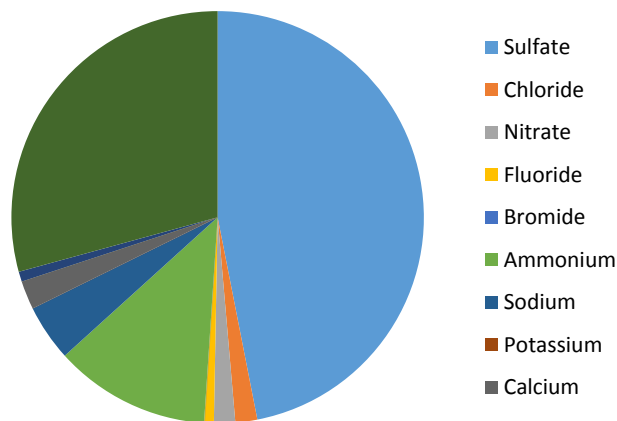**Fig. 7.** Average contribution of ion to condensable inorganic PM$_{2.5}$ mass measured using Method 201A/5.1 from the AAC laboratory.

et al., 2014). Total PM$_{2.5}$ emissions measured using Methods 201A/202 were 20% lower than those measured using Methods 201A/5.1. For both methods, the condensable inorganic fraction was by far the largest fraction of the PM$_{2.5}$.

3.3. Gaseous emissions

We monitored O$_2$, CO$_2$, NO$_x$ and CO in the NGT exhaust (Summary data shown in Table 2). Measurements were taken from a stationary point in the stack throughout the PM$_{2.5}$ testing. The data shows that O$_2$ levels were generally between 13.0 and 13.1%, except during the two test days with the greatest number of turbine load changes on which it increased to 13.3%. As expected, CO$_2$ levels tracked O$_2$ levels. NO$_x$ emissions averaged 2.1 ppmc (ppmc = ppm, dry corrected to 15% O$_2$). CO emissions averaged 1.0 ppmc, with daily averages varying from 0.7 to 1.3 ppmc.

Ammonia (NH$_3$) slip tests were performed to determine whether the turbine was injecting the correct amount of NH$_3$ into the SCR unit. Measurements were made at each of the 12 sample

Table 1
Summary of PM$_{2.5}$ emissions measurements using Method 201A/5.1.

PM	Avg, gr/dscf (μg/m^3)	Stdev	RMS	Uncertainty at 99% C.L.	Uncertainty, %	LOD	Percent of total PM
Solid>2.5 μm	2.30E-05 (52.63)	1.40E-05	60.1	1.60E-05	70.4	4.20E-05	
Solid<2.5 μm	2.10E-05 (48.06)	1.00E-05	50.0	1.20E-05	58.6	3.10E-05	7.1
Condensible inorganic<2.5 μm	2.51E-04 (574.37)	4.60E-05	18.5	5.40E-05	21.7	1.39E-04	84.8
Condensible organic<2.5 μm	2.40E-05 (54.92)	1.40E-05	58.7	1.70E-05	68.8	4.20E-05	8.1
Total <2.5 μm	2.96E-04 (677.35)	5.80E-05	19.5	6.80E-05	22.8	1.73E-04	

Table 2
Summary of gaseous emissions, ammonia slip measurements, & SO_2/SO_3 (Daily data can be seen in the supplementary file).

O_2, % dry	CO_2, % dry	NO_x, ppm dry	CO, ppm dry	NH_3, ppm flue gas	SO_2, ppm dry	SO_3, ppm dry	SO_3/SO_x ratio, %	Moisture fraction
		NO_x, ppm @ 15% O_2	CO, ppm @ 15% O_2	NH_3, ppm @15% O_2	SO_2, ppm dry @ 15% O_2	SO_3 ppm dry @ 15% O_2		
13.11	4.44	2.74	1.35	4.8	0.060	0.017	23	0.108
		2.07	1.02	3.6	0.045	0.013		

points, and samples were taken for 5 min at each point. NH_3 slip measured in the stack averaged 4.8 ppm, or 3.6 ppmc, in compliance with permit conditions. NH_3 slip for a GT SCR system with a 5 ppm slip end of life guarantee (like the one in the Walnut Creek facility) will be near zero (i.e., less than 0.1 ppm) at start-up, if the system was properly designed and the AIG (ammonia injection grid) has been tuned. The average measured slip of 3.6 ppmc would be expected at over 80% of the catalyst's life (i.e., greater than 80,000 operating hours). NH_3 slip higher than usual for a new combined cycle SCR system was possibly due to a NH_3 slip imbalance entering the catalyst, some flue gas bypassing the catalyst, or low catalyst volume.

SO_x were measured because of their ability to form sulfuric acid in the atmosphere. The SO_x triplicate tests were performed (one per day) on three days with target run times of 8 h. All of the SO_x were created by the oxidation of sulfur compounds present in the natural gas when it was burned. Measured SO_2 emissions averaged 0.060 ppm. When corrected to 15% O_2, SO_2 emissions averaged 0.045 ppmc. Measured SO_3 emissions averaged 0.017 ppm at the stack. SO_3 emissions averaged 0.013 ppmc. SO_3 accounted for an average of 23% of the total SO_x emissions. SO_2 is a dominant species under both fuel lean and even fuel rich combustion conditions. SO_3 concentrations are usually higher than equilibrium calculations (due to slow reaction to reduce SO_3 to SO_2), and are usually in the range of few percentages of SO_x emissions (Glassman and Yetter, 2007). A report by GE (Pavri and Moore, 2001) shows about 95% of SO_x is SO_2. While some of the SO_3 was formed in the combustion process, it is likely that more was formed as the SO_2 (a product of combustion) passed across the oxidizing CO and SCR catalysts. If we assume that all of the 0.060 ppm SO_x (at STP T = 298 K) measured in the exhaust was converted from sulfur in the fuel then there is about 0.34 grain/100scf of sulfur in the fuel, this is within the average range of sulfur concentrations for California pipeline natural gas (0.25–1 grain/100scf).

4. Discussion and conclusion

NGTs currently supply over half of the electricity used in California and this percentage has been increasing due to a decrease of hydroelectric and nuclear power generation. This study furthers our understanding of particle size distributions and the nature of particles at different modes for this NGT and results may not apply to all NGTs.

After turbine exhaust was diluted sevenfold with filtered air, particle concentrations in the 10–300 nm size range were approximately two orders of magnitude higher than those in the ambient air and those in the 2–3 nm size range were up to four orders of magnitude higher. The ambient air PM mass calculated from the SMPS data was in the range of the AQI PM mass reported that day for the region. Ambient air particle concentrations were slightly higher than average urban Southern California levels due to the test site being located next to a train yard and near a major highway. The loading of $PM_{2.5}$ in the exhaust, measured using Method 201A/5.1, was 0.000296 grain/dscf (677 µg/m^3). Of the total

$PM_{2.5}$: 8.1% was condensable organic PM, 84.8% was condensable inorganic PM, and 7.1% was solid PM, and PM mass calculated by the SMPS data was within a factor of three compared to the mass reported by Method 201A/5.1.

This study found that the exhaust from the turbine contained higher concentrations of nanoparticles than they were present in ambient air. Further research to determine the nature and volatility of the (sub-10 nm) ultrafine particles observed in this study is essential to understand their potential harm to human health.

Acknowledgments

Appendix A. Supplementary data

Supplementary data related to this article can be found at http://dx.doi.org/10.1016/j.atmosenv.2015.11.048.

References

Abdul-Khalek, I., 1996. Online Measurement of Volatile and Solid Exhaust Particles Using a Catalytic Stripper System: Characterization and Application, Mechanical Engineering. Masters thesis. University of Minnesota.

Abdul-Khalek, I.S., Kittelson, D.B., 1995. Real Time Measurement of Volatile and Solid Exhaust Particles Using a Catalytic Stripper. SAE Technical Paper 950236. http://dx.doi.org/10.4271/950236.

Buseck, P.R., Adachi, K., 2008. Nanoparticles in the atmosphere. Elements 4, 389–394.

CEC, 2008. Walnut Creek Energy Park.

CEC, 2014. Calfornia Energy Commission Energy Alamanac, California Electrical Energy Generation, Total Production, by Resource Type (Gigawatt Hours).

Chang, M., England, G., 2004. Development of Fine Particulate Emission Factors and Speciation Profiles for Oil and Gas-fired Combustion Systems. Other Report: Pilot-Scale Dilution Sampler Design and Validation Tests (Laboratory Study). California Energy Commission.

EIA, 2013a. Annual Energy Outlook 2013 with Projections to 2040.

EIA, 2013b. Updated Capital Cost Estimates for Utility Scale Electricity Generating Plants.

Elder, A., Oberdörster, G., 2005. Translocation and effects of ultrafine particles outside of the lung. Clin. Occup. Environ. Med. 5, 785–796.

England, G., 2004. Development of Fine Particulate Emission Factors and Speciation Profiles for Oil and Gas-Fired Combustion Systems. Topical Report: Impact of Operating Parameters on Fine Particulate Emissions from Natural Gas-Fired Combined Cycle and Cogeneration Power Plants. California Energy Commission.

England, G., McGrath, T., 2004. Development of Fine Particulate Emission Factors and Speciation Profiles for Oil and Gas-Fired Combustion Systems. Topical Report: Test Results for a Cogeneration Plant with Supplementary Firing, Oxidation Catalyst, and SCR at Site Golf. California Energy Commission.

England, G., Wien, S., McGrath, T., Hernandez, D., 2004. Development of Fine Particulate Emission Factors and Speciation Profiles for Oil and Gas-Fired Combustion Systems. Topical Report: Test Results for a Cogeneration Plant with

Supplementary Firing, Oxidation Catalyst, and SCR at Site Echo. California Energy Commission.

England, G.C., Watson, J.G., Chow, J.C., Zielinska, B., Chang, M.-C.O., Loos, K.R., Hidy, G.M., 2007. Dilution-based emissions sampling from stationary sources: part 1-compact sampler methodology and performance. J. Air Waste Manag. Assoc. 57, 65—78.

EPA, 2010. Method 201A-determination of PM10 and PM2.5 emisssions from stationary sources (constant sampling rate procedure). In: EPA, U.S. (Ed.), 40 CFR Part 51 Appendix M.

EPA, 2015. AP-42, Compilation of Air Pollutant Emission Factors.

FERCo, UCI, UCR, Environ, AET, 2009. Control Strategies and Technologies for Particulate Matter under 2.5 Microns and Ultrafine Particulate Emissions from Natural Gas-Fired Turbine Power Plants. Phase 1-Technical Assessment. South Coast Air Quality Management District.

FERCo, Delta, UCR, 2014. Control Strategies and Technologies for Particulate Matter under 2.5 Microns and Ultrafine Particulate Emissions from Natural Gas-Fired Turbine Power Plants. Phase 2-GE LMS100 Test Results. South Coast Air Quality Management District.

Friedlander, S.K., 2000. Smoke, Dust, and Haze: Fundamentals of Aerosol Dynamics, second ed. Oxford University Press.

GE, 2015. General Electric Water and Power, Fast, Flexible Power. Aeroderivative Product and Services Solution.

Glassman, I., Yettter, R.A., 2007. Combustion, fourth ed. Academic Press. ISBN-10: 0120885735.

Grady, M., Jung, H., Kim, Y., Park, J., et al., 2013. Vehicle Cabin Air Quality with Fractional Air Recirculation. SAE Technical Paper 2013-01-1494. http://dx.doi.org/10.4271/2013-01-1494.

Gysel, N., Welch, W., Chen, C.-L., Miller, W., Cocker, D., 2015. Development of New PM Test Protocol and Characterization of PM Formation and Growth from Natural Gas Turbine Emissions (p. in preparation).

HEI, 2013. Understanding the Health Effects of Ambient Ultrafine Particles, HEI Perspectives 3. Health Effect Institute, Boston, MA.

Herndon, S.C., Jayne, J.T., Lobo, P., Onasch, T.B., Fleming, G., Hagen, D.E., Whitefield, P.D., Miake-Lye, R.C., 2008. Commercial aircraft engine emissions characterization of in-use aircraft at Hartsfield-Jackson Atlanta International Airport. Environ. Sci. Technol. 42, 1877—1883.

Klippel, N., Kasper, M., Bengtsson, K., 2002. Gas turbines-sources or sinks for ambient air aerosol?. In: 6th ETH Conference on Nanoparticle Measurement. Switzerland, Zurich.

Klippel, N., Wood, T., Pearce, B., Bengtsson, K., Kasper, M., Mosimann, T., 2004. On-line Measurement of Ultrafine Particle Emissions from Gas Turbines (Technical report ALSTOM Power).

Kuwata, M., Zorn, S.R., Martin, S.T., 2011. Using elemental ratios to predict the density of organic material composed of carbon, hydrogen, and oxygen. Environ. Sci. Technol. 46, 787—794.

Lobo, P., Hagen, D.E., Whitefield, P.D., 2011. Comparison of PM emissions from a commercial jet engine burning conventional, biomass, and Fischer—Tropsch fuels. Environ. Sci. Technol. 45, 10744—10749.

Maricq, M.M., Xu, N., 2004. The effective density and fractal dimension of soot particles from premixed flames and motor vehicle exhaust. J. Aerosol Sci. 35, 1251—1274.

Mohr, M., Ylätalo, S., Riccius, O., Kauppinen, E.I., 1995. Formation of ultrafine particles inside an electrostatic precipitator caused by interaction of denitrification unit and corona discharge. J. Aerosol Sci. 26, S871—S872.

Murphy, S.M., Agrawal, H., Sorooshian, A., Padró, L.T., Gates, H., Hersey, S., Welch, W., Jung, H., Miller, J., Cocker III, D.R., 2009. Comprehensive simultaneous shipboard and airborne characterization of exhaust from a modern container ship at sea. Environ. Sci. Technol. 43, 4626—4640.

Nakao, S., Tang, P., Tang, X., Clark, C.H., Qi, L., Seo, E., Asa-Awuku, A., Cocker, D., 2013. Density and elemental ratios of secondary organic aerosol: application of a density prediction method. Atmos. Environ. 68, 273—277.

Nguyen, A., Jung, H., 2015. Influence of Wind and Driving Conditions on Self-polluting Tailpipe Emissions (p. in preparation).

Pavri, R., Moore, G., 2001. Gas Turbine Emissions and Control. GE Power Systems. URL: https://powergen.gepower.com/content/dam/gepower-pgdp/global/en_US/documents/technical/ger/ger-4211-gas-turbine-emissions-and-control.pdf.

SCAQMD, 1989. Method 5.1 determination of particulate matter emissions from stationary sources using a wet Impingement train. In: District, S.C.A.Q.M. (Ed.).

SCAQMD, 2002. Rule 1303. In: District, S.C.A.Q.M. (Ed.).

Schmatloch, V., 2000. Fine Particle Emissions from Wood and Oil Fired Furnaces, 4th ETH Conference on Nanoparticle Measurement. Switzerland, Zurich.

Sewell, A., 2013. Activists praise San Onofre closure, but 1,100 layoffs expected. LA Times.

Stenitzer, M., 2003. Nano Particle Formation in the Exhaust of Internal Combustion Engines. Masters thesis. Vienna Technical University.

Tamura, T., 2013. Gap analysis for the stationary combustion filterable and condensible particulate matter emission factors. Tetra Tech. Petrol. Technol. Alliance Can.

TSI, 2012. Electrical Aerosol Detector Model, 3070A.

Wey, C.C., Anderson, B.A., Wey, C., Miake-Lye, R.C., Whitefield, P., Howard, R., 2007. Overview on the aircraft particle emissions experiment (APEX). J. Propuls. Power 23, 898—905.

Wien, S., England, G., Chang, M., 2004. Development of Fine Particulate Emission Factors and Speciation Profiles for Oil and Gas-Fired Combustion Systems. Topical Report: Test Results for a Cogeneration Plant with Supplementary Firing, Oxidation Catalyst, and SCR at Site Bravo. California Energy Commission.

Wilson, W.E., Stanek, J., Han, H.-S., Johnson, T., Sakurai, H., Pui, D.Y., Chen, D.-R., Duthie, S., 2007. Use of the electrical aerosol detector as an indicator of the surface area of fine particles deposited in the lung. J. Air Waste Manag. Assoc. 57, 211—220.

Zheng, Z., Durbin, T.D., Karavalakis, G., Johnson, K.C., Chaudhary, A., Cocker III, D.R., Herner, J.D., Robertson, W.H., Huai, T., Ayala, A., 2012. Nature of Sub-23-nm particles downstream of the european particle measurement programme (PMP)-compliant system: a real-time data perspective. Aerosol Sci. Technol. 46, 886—896.

Zhu, Y., Eiguren-Fernandez, A., Hinds, W.C., Miguel, A.H., 2007. In-cabin commuter exposure to ultrafine particles on Los Angeles freeways. Environ. Sci. Technol. 41, 2138—2145.